

Investigation of a New Red-Emitting, Eu^{3+} -Activated MgAl_2O_4 Phosphor[†]

Vijay Singh, MD, Masuqul Haque, and Dong-Kuk Kim*

Department of Chemistry, College of Natural Sciences, Kyungpook National University, Daegu 702-701, Korea

*E-mail: kindk@knu.ac.kr

Received July 6, 2007

$\text{MgAl}_2\text{O}_4:\text{Eu}^{3+}$ red-light emitting powder phosphor was prepared at temperature as low as 500 °C within a few minutes by using the combustion route. The prepared powder was characterized by X-ray diffraction, scanning electron microscopy and Fourier-transform infrared spectrometry. The luminescence of Eu^{3+} -activated MgAl_2O_4 shows a strong red emission dominant peak around 611 nm, which can be attributed to the ${}^5\text{D}_0\text{-}{}^7\text{F}_2$ transition of Eu^{3+} ions from the synthesized phosphor particles under excitation (394 nm). Electron paramagnetic resonance (EPR) measurements at the X-band showed that no signal could be attributed to Eu^{2+} ions in MgAl_2O_4 .

Key Words : Combustion, Dopant, Phosphor, Photoluminescence, Electron spin resonance

Introduction

Recently, many aluminate materials have been extensively studied as phosphors for the next generation of display and lighting devices. Among them, magnesium-aluminum oxide (MgAl_2O_4) spinel crystals with related transition dopants have received a great deal of attention due to its mechanical strength, high resistance to chemical attacks, and its outstanding dielectric and optical properties.¹⁻⁴ The spinel crystals (MgAl_2O_4) that were doped with transition metal ions such as Ni^{2+} , Cr^{3+} , Fe^{3+} , Co^{3+} , have been studied by various groups.⁵⁻⁷ Recently, we have reported that there are two independent emission channels in Mn-doped MgAl_2O_4 phosphors.⁸

Luminescent materials with related Eu^{3+} dopants have been extensively used in optical fields including lasers, electroluminescent devices and oscillators. Similarly, many series of Eu^{3+} -doped materials have been synthesized and their optical properties have been evaluated.⁹⁻¹² In recent years, a number of publications related to the synthesis and properties of europium-doped aluminates have appeared, for example $\text{Eu}^{2+}/\text{Eu}^{3+}$ emissions were studied in $\text{Sr}_3\text{Al}_2\text{O}_6$,¹³ $\text{Sr}_4\text{Al}_{14}\text{O}_{25}$, CaAl_2O_9 , $\text{BaMgAl}_{10}\text{O}_{17}$ and ZnAl_2O_4 .¹³⁻¹⁶ Similar to sulfides,¹⁷ which have been widely used as phosphor hosts in the past, alkaline earth aluminates are currently being used in a variety of applications as they are chemically stable in ambient environments.¹⁸

MgAl_2O_4 has been selected as the host material in this work. During the past few years, non rare-earth doped MgAl_2O_4 aluminates received much attention because of their applicability regarding solid-state optical devices, however, rare-earth doped MgAl_2O_4 aluminates have received little attention. The aluminate of interest in the present study is the Eu -doped MgAl_2O_4 .

In the past, MgAl_2O_4 has been prepared by solid state reactions,¹⁹ which usually demand high annealing temper-

atures and long reaction times. Low temperature and less time consuming methods will provide great commercial impact. We have succeeded in the production of Eu -doped MgAl_2O_4 spinel powders by a low-temperature process and the results are reported herein. This method, the combustion process, involves low furnace temperatures and it can be carried out within 5 minutes. The prepared combustion product was characterized by using techniques such as powder X-ray diffraction (XRD), scanning electron microscopy (SEM), Fourier transform infrared (FT-IR) spectra, photoluminescence (PL) and electron paramagnetic resonance (EPR).

Experimental

Eu^{3+} doped crystals aluminates were prepared by the formula $\text{Mg}_{0.99}\text{Eu}_{0.01}\text{Al}_2\text{O}_4$ [with the source materials of 1.6916 g $\text{Mg}(\text{NO}_3)_2 \cdot 6\text{H}_2\text{O}$, 5 g $\text{Al}(\text{NO}_3)_3 \cdot 9\text{H}_2\text{O}$, 2.6690 g urea and 0.0117 g Eu_2O_3]. For the combustion synthesis of MgAl_2O_4 , metal nitrates are used as oxidizers, and urea is employed as fuel. These ratios determine the total oxidation (O) and reduction (F) valencies of the components, so that the equivalence ratio O/F is unified, when the energy released by the combustion is at its maximum.²⁰

Starting materials were crushed and ground in an agate mortar to form paste. The paste was transferred into a ceramic crucible, which was then introduced into a muffle furnace maintained at 500 ± 10 °C. Initially, the paste melted and underwent a dehydration process. This was followed by decomposition with the evolution of large amounts of gas. The mixture was then frothed and swelled thus forming a foam which ruptured with a flame and glowed to incandescence. During incandescence, the foam further swelled to the capacity of the container. The entire combustion process was completed in less than 5 min. The dish was taken out and the foamy product was crushed into a fine powder. This powder was white in colour and its properties were evaluated.

[†]This paper is dedicated to Professor Sang Chul Shim on the occasion of his honorable retirement.

A powder-phase analysis was done using XRD. The diffractogram was recorded (X'pert, Philips) using Cu K α radiation ($\lambda = 0.15418$ nm) in the 2θ range between 10° and 70° . Particle morphologies were observed using a scanning electron microscope (JSM-5610LV, JEOL). FT-IR spectra were taken using a Perkin-Elmer Rx1 instrument in the range 4000 – 400 cm^{-1} . Photoluminescence measurements were carried out at room temperature on a Shimadzu RF-5301 PC spectrophotometer. EPR measurements were conducted using a Bruker EMX 10/12 X-band ESR spectrometer.

Results and Discussion

X-ray diffraction. The X-ray diffraction (XRD) pattern of the as-prepared $\text{Mg}_{0.99}\text{Eu}_{0.01}\text{Al}_2\text{O}_4$ is shown in Figure 1a. The observed diffraction peaks matched the standard MgAl_2O_4 spinel (JCPDS, No. 77-0435; Figure 1b). These diffraction peaks can be indexed as (111), (220), (311), (222), (440), (422), (511), (440) and (531). The ratios of peak intensities (standard and prepared powder) were determined to be the same. As the XRD indicated, the prepared materials were fully crystalline. Therefore, further heat-treatment for crystallization is not required.

Scanning electron microscopy. SEM micrographs of the as-prepared powder are shown in Figure 2. It is clear from Figure 2a that the particles are angular and of varying sizes; some regions contain pores while some do not. Figure 2b shows several non-uniform pores within these crystals and

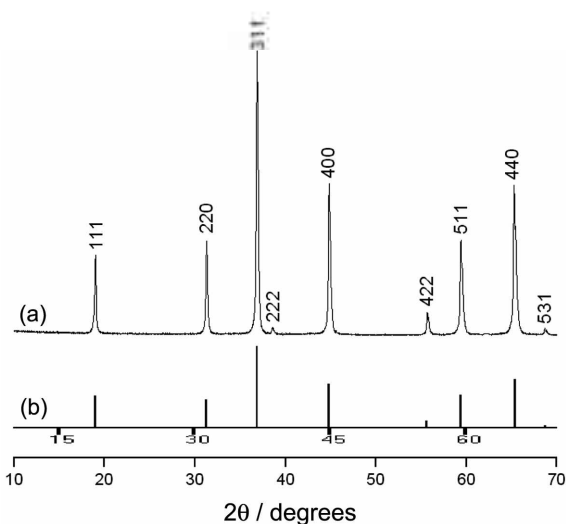


Figure 1. Powder XRD patterns of (a) $\text{MgAl}_2\text{O}_4:\text{Eu}$ and (b) MgAl_2O_4 diffraction pattern (JCPDS, No. 77-0435).

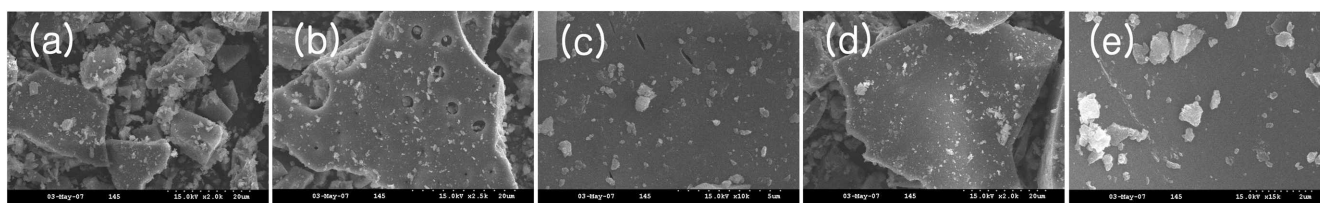


Figure 2. SEM images of $\text{MgAl}_2\text{O}_4:\text{Eu}$.

the pore diameter ranged between 600 nm and 2 μm . This non-uniformity is caused by the non-uniform distribution of temperature and mass flow during combustion. High magnification (Figure 2c) images show that there are several small particles within a crystal and that there are some cracks on the surface.

It is believed that these cracks and the type of porosity are formed because large amounts of gas escaped during combustion reactions. There are some angular crystals which do not have cracks or porosity (shown in Figure 2d). Figure 2e is a magnified view of Figure 2d. From these figures, it is clear that several nanoparticles can be seen. By this method, it is possible to produce phosphor nanocrystals along with the incorporation of a dopant in its lattice. It should be pointed out that the morphology of the undoped MgAl_2O_4 and Eu-doped MgAl_2O_4 samples (in this work) are almost the same.⁸ This could be due to the addition of a very low amount of dopant.

FT-IR studies. The FT-IR spectrum of the Eu-doped MgAl_2O_4 phosphor is shown in Figure 3. The band at 3432 cm^{-1} can be assigned to the vibration mode of chemically-bonded hydroxyl groups. The band at 1622 cm^{-1} corresponds to the deformation vibration of water (δ_{OH}) molecules. Two sharp peaks at 696 and 533 cm^{-1} are due to the stretching mode of Al-O in an octahedral coordination state (AlO_6 octahedral units), which must have come from MgAl_2O_4 . Quite similar to the XRD results (Figure 1a), the FT-IR also showed sharp and distinct Al-O bands indicating that any post-treatment for crystallization is not necessary.

Photoluminescence studies. Rare-earth ions are known to exist in various valence states although the trivalent state is the most prevalent. In particular, Eu ions are known to be stable in trivalent as well as divalent states. The excitation

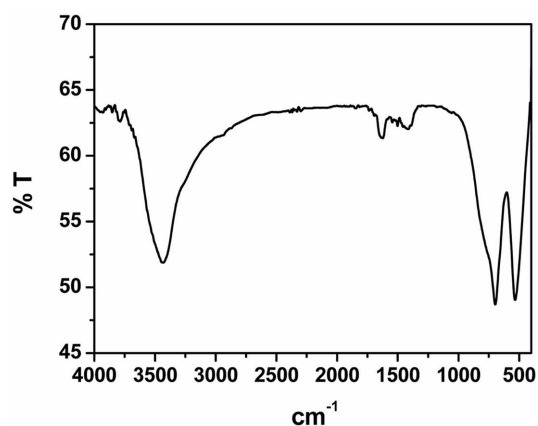


Figure 3. FT-IR spectra of $\text{MgAl}_2\text{O}_4:\text{Eu}$ at room temperature.

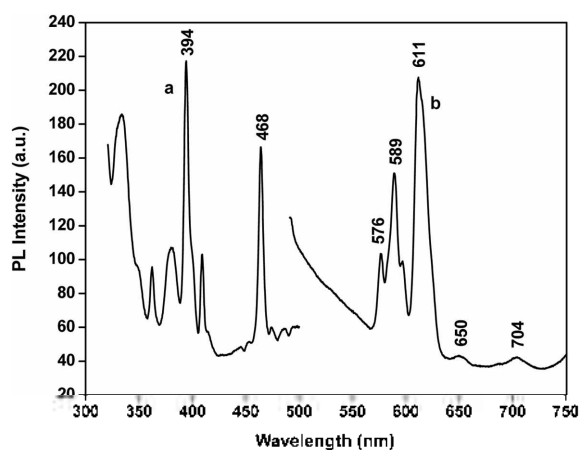


Figure 4. Photoluminescence spectra of $\text{MgAl}_2\text{O}_4:\text{Eu}$: (a) excitation spectra ($\lambda_{\text{em}} = 611 \text{ nm}$) and (b) emission spectra ($\lambda_{\text{ex}} = 394 \text{ nm}$).

spectra for Eu^{3+} phosphors in MgAl_2O_4 (Figure 4) present a maximum at 394 nm, which is ascribed to the $^5\text{L}_6$ level of Eu^{3+} .²¹ The emission spectra (Figure 4) of the compounds obtained present characteristic Eu^{3+} emission transitions arising mainly from the $^5\text{D}_0$ level to the $^7\text{F}_J$ ($J = 0, 1, 2, 3, 4$) manifolds.²² In the emission spectra, the band corresponding to the $^5\text{D}_0 \rightarrow ^7\text{F}_2$ transition has a larger amplitude than that of $^5\text{D}_0 \rightarrow ^7\text{F}_1$, which is an indication that the symmetry around Eu^{3+} does not contain a centre of inversion.²³ The presence of the $^5\text{D}_0 \rightarrow ^7\text{F}_2$ transition indicates that Eu^{3+} is located in one of the C_m , C_n or C_s symmetry groups.²⁴ The relatively weak emission peaks of Eu^{3+} ions around 589 nm, corresponding to the $^5\text{D}_0 \rightarrow ^7\text{F}_1$ magnetic dipole transition, compared to the peak at 611 nm corresponding to the induced electric dipole transition, clearly indicate a lower symmetry for Eu^{3+} ions in these aluminates. No broad emissions attributable to Eu^{2+} emission could be seen in the emission spectra (shown in Figure 4), indicating that the reduction of Eu^{3+} ions could not be achieved in MgAl_2O_4 phosphor.

The PL peak of the $\text{Mg}_{0.99}\text{Eu}_{0.01}\text{Al}_2\text{O}_4$ phosphors is due to Eu^{3+} ions. The PL peak position of the $\text{Mg}_{0.99}\text{Eu}_{0.01}\text{Al}_2\text{O}_4$ phosphors is considered to result from the crystal structures of the host materials. MgAl_2O_4 with a spinel structure, Mg^{2+} ions, occupy tetrahedral sites while Al^{3+} ions occupy octahedral lattice sites. The emission spectra of Eu^{3+} ions in MgAl_2O_4 (for excitation at 394 nm) contain both 589 nm and 611 nm peaks. The first peak corresponds to the magnetic dipole transition, while the second peak, which corresponds to the induced electric dipole transition, can be observed when there is a deviation from inversion symmetry. The presence of both peaks indicates that Eu^{3+} ions probably occupy octahedral Al^{3+} sites. If Eu^{3+} ions occupied tetrahedral Mg^{2+} sites without inversion symmetry, the intensity of the 589 nm peak would have been dominant.

Electron paramagnetic resonance studies. The EPR spectra of Eu doped and undoped MgAl_2O_4 aluminates are shown in Figure 5. The EPR spectrum of $\text{MgAl}_2\text{O}_4:\text{Eu}$, shown in Figure 5a, contained a broad signal around 3300 G along with another signal at 1650 G ($g = 4.8$). It is to be noted

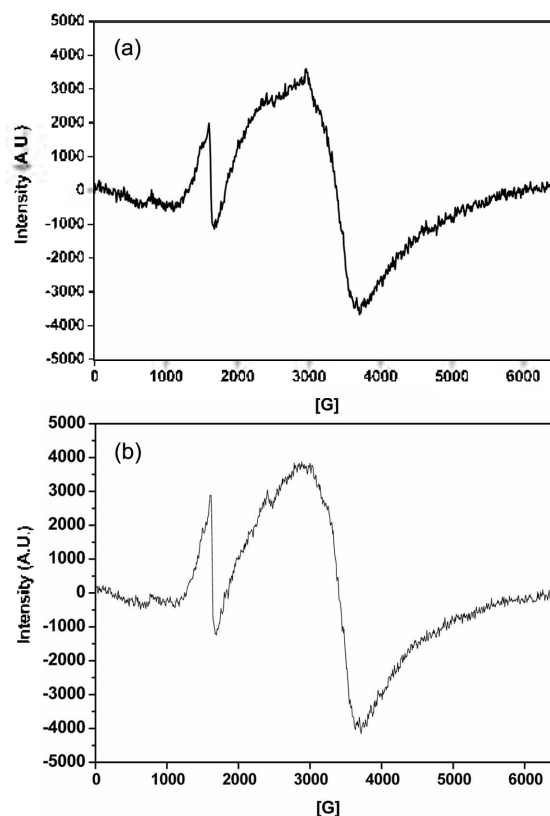


Figure 5. EPR spectra of (a) $\text{MgAl}_2\text{O}_4:\text{Eu}$ and (b) MgAl_2O_4 .

that these signals were also present in the EPR spectrum of the undoped MgAl_2O_4 (Figure 5b), indicating that they are from some unintentional impurity ions. The signal at 1650 G has been attributed to low symmetry Fe^{3+} ions.²⁵ The Fe^{3+} impurity ions in our samples must have occurred from starting materials. These iron compounds were not detected in the XRD because they were in very low quantities however; it was difficult to assign the central broad line around 3300 G. No signal, attributable to Eu^{2+} , could be observed in $\text{MgAl}_2\text{O}_4:\text{Eu}$. The PL emission in the red region had already indicated the presence of Eu as Eu^{3+} ions in the prepared MgAl_2O_4 samples. This is further confirmed by the EPR spectra that there is no signal due to Eu^{2+} ions.

Conclusions

The preferred route of synthesis for doped MgAl_2O_4 ceramic phosphors has commonly happened to be the solid state reactive firing of the appropriated amounts of MgO and Al_2O_3 with the dopant oxide. Nevertheless, this conventional technique of ceramic manufacture required temperatures well above 1000 °C for prolonged firing times typically in the vicinity of 24 h to form the single-phase, spinel phosphor phase. Our experiments revealed that urea-nitrate combustion synthesis has outstanding potential for producing Eu-doped MgAl_2O_4 red-emitting phosphors in a single step. The mono phase of Eu-doped MgAl_2O_4 could be obtained at low temperature without any post-calcination treatment. The prepared phosphor consisted of nano crystals. The FT-IR

revealed the presence of Al-O bands indicating the formation of the MgAl_2O_4 phase. These results, though preliminary in nature, suggest that Eu^{3+} -doped MgAl_2O_4 phosphors have the potential to be used as red-emitting phosphors in preparing display devices. The advantages of the combustion synthesis process are that it is a simple procedure; less time is needed, it can be conducted at low temperature, and the starting materials are inexpensive.

Acknowledgment. This work was supported by the Ministry of Commerce, Industry and Energy of Korea through a Components and Materials Technology Development project (No. 0401-DD2-0163).

References

1. Donegan, J. F.; Bergin, F. J.; Glynn, T. J.; Imbush, G. F.; Remeika, J. P. *J. Lumin.* **1986**, *35*, 57.
2. Garapon, C.; Manaa, H.; Moncoge, R. *J. Chem. Phys.* **1991**, *95*, 5501.
3. Ibarra, A.; Vila, R.; Garner, F. A. *J. Nucl. Mater.* **1996**, *233*, 1336.
4. Tomita, A.; Sato, T.; Tanaka, K.; Kawabe, Y.; Shirai, M.; Hanamura, E. *J. Lumin.* **2004**, *109*, 19.
5. Kuleshov, N. V.; Sheherbitsky, V. G.; Mikhailov, V. P.; Kuck, S.; Koetke, J.; Petermann, K.; Huber, G. *J. Lumin.* **1997**, *71*, 265.
6. Rossi, F.; Pucker, G.; Montagna, M.; Ferrari, M.; Boukenter, A. *Opt. Mater.* **2000**, *13*, 373.
7. Carvalhaes, R. P. M.; Rocha, M. S.; de Souza, S. S.; Blak, A. R. *Nucl. Instrum. Methods Phys. Res., Sect. B* **2004**, *218*, 158.
8. Singh, V.; Chakradhar, R. P. S.; Rao, J. L.; Kim, D.-K. *J. Solid State Chem.* **2007**, *180*, 2607.
9. Ishizaka, T.; Kurokawa, Y. *J. Appl. Phys.* **2001**, *90*, 243.
10. Guo, P. M.; Zhao, F.; Li, G. B.; Liao, F. H.; Tian, S. J.; Jing, X. P. *J. Lumin.* **2003**, *105*, 61.
11. Liang, H.; Zhang, Q.; Zheng, Z. Q.; Ming, H.; Li, Z. C.; Xu, J.; Chen, B.; Zhao, H. *Opt. Lett.* **2004**, *29*, 477.
12. Xiao, X. Z.; Yan, B. *J. Alloys Compd.* **2007**, *433*, 246.
13. Mingying, P.; Ning, D.; Yanbo, Q.; Baotao, W.; Chen, W.; Danping, C.; Jianrong, Q. *J. Rare Earths* **2006**, *24*, 749.
14. Singh, V.; Rao, T. K. G.; Zhu, J.-J. *J. Lumin.* **2007**, *126*, 1.
15. Chang, H.; Lenggono, I. W.; Ogi, T.; Okuyama, K. *Mater. Lett.* **2005**, *59*, 1183.
16. Yang, C.-C.; Chen, S.-Y.; Cheng, S.-Y. *Powder Technol.* **2004**, *148*, 3.
17. Jia, D.; Wu, B.; Zhu, J. *J. Lumin.* **2000**, *90*, 33.
18. Park, B.-K.; Lee, S.-S.; Kang, J.-K.; Byeon, S.-H. *Bull. Kor. Chem. Soc.* **2007**, *28*, 1467.
19. Bratton, R. J. *J. Am. Ceram. Soc.* **1971**, *52*(8), 141.
20. Jain, S. R.; Adiga, K. C.; Vernekar, V. R. P. *Combust. Flame* **1981**, *40*, 71.
21. Serra, O. A.; Thompson, L. C. *Inorg. Chem.* **1976**, *15*, 504.
22. Ribeiro, S. J. L.; Dahmouche, K.; Ribeiro, C. A.; Santilli, C. V.; Pulcinelli, S. H. *J. Sol-Gel Sci. Tech.* **1998**, *13*, 427.
23. Jorgensen, C. K.; Reisfeld, R. *J. Less-Common Met.* **1983**, *93*, 107.
24. Porcher, P. *Rare Earths*; Saez, R.; Caro, P. A., Eds.; Madrid, 1998; p 43.
25. Dowsing, R. D.; Gibson, J. F. *J. Chem. Phys.* **1969**, *50*, 294.